Early Holocene environment on Bjørnøya (Svalbard) inferred from multidisciplinary lake sediment studies

BARBARA WOHLFARTH, GEOFFREY LEMDAHL, SIV OLSSON, THOMAS PERSSON, IAN SNOWBALL, JONAS ISING and VIV JONES

Wohlfarth, B., Lemdahl, G., Olsson, S., Persson, T., Snowball, I., Ising, J. & Jones, V. 1995: Early Holocene environment on Bjørnøya (Svalbard) inferred from multidisciplinary lake sediment studies. *Polar Research 14(2)*, 253–275.

Bjørnøya, a small (178 km^2) island situated between the mainland of Norway and southern Spitsbergen, provides the opportunity for the reconstruction of early Holocene terrestrial and limnic palaeoenvironments in the southwestern Barents Sea. The AMS ^{14}C dating technique, geochemical, mineral magnetic, micro- and macrofossil analyses were applied to sediments recovered from lake Stevatnet and the results are interpreted in terms of palaeoenvironmental conditions between 9800 and 8300 ^{14}C BP. After the disappearance of local glaciers before ca 9800 ^{14}C BP, the lake productivity increased rapidly at the same time as pioneer plant communities developed on soils which gradually became more stable. Insect data indicates that strong seasonal contrasts with mean July temperatures around 9°C and mean January temperatures around −12°C prevailed between 9500 and 8300 ^{14}C BP. These high summer temperatures, possibly as much as 4–5°C higher than the present, favoured the development of a flora including *Dryas* and *Angelica* cf. *archangelica*. The enhanced freeze/thaw processes led to an increased erosion of minerogenic and organic material. After 8000 ^{14}C BP the temperatures may have gradually declined. The environmental reconstruction derived from our data set supports the conceptual insolation model which proposes maximum Holocene seasonality for the Northern Hemisphere at ca 9000 ^{14}C BP.

Barbara Wohlfarth, Geoffrey Lemdahl, Siv Olsson, Thomas Persson, Ian Snowball and Jonas Ising, Department of Quaternary Geology, Tornavägen 13, S-22363 Lund, Sweden; Viv Jones, Department of Geography, University College London, 26 Bedford Way, London WC1H 0AP, U.K.

Introduction

The island of Bjørnøya is situated in the southwestern Barents Sea, between the mainland of Norway and the southern end of Svalbard (Fig. 1A). During the last Glacial maximum (ca 18,000 ^{14}C BP), the Barents Sea ice sheet reached west to the continental shelfbreak and a glacier, possibly dry-based, covered Bjørnøya (Elverhøi & Solheim 1983; Vorren et al. 1988; Elverhøi et al. 1990; Vorren 1992; Elverhøi et al. 1995). The ice receded in two steps, firstly at ca 14,800 ^{14}C BP from the outer shelf and the southwestern Barents Sea and secondly at ca 13,000–12,000 ^{14}C BP from the inner and shallower shelf (Elverhøi et al. 1995). These separate recessions correspond to meltwater signals recorded in marine cores between 15,000–13,000 ^{14}C BP (Hald & Dokken 1995). The timing of the decay of the Barents Sea ice sheet is also indicated by an influx of meltwater from major Siberian rivers into the central Arctic Ocean slightly before 14,500 ^{14}C BP (Stein et al. 1994). At ca 12,500 ^{14}C BP the first warming of the ocean surface is recorded in marine sediment cores from the continental margin off western Svalbard and the western Barents Sea (Hald & Dokken 1995). Mollusc dates from the northern Barents Sea, and emergence curves from Kong Karls Land, indicate that the Barents Sea ice sheet had disappeared by ca 10,000 ^{14}C BP (Salvigsen 1981; Elverhøi et al. 1990; Bondevik et al. 1995; Hjort et al. 1995). This date agrees well with oxygen isotope data from marine cores which show a rapid temperature increase of 2–3°C between 10,000–9500 ^{14}C BP (Hald & Dokken 1995) and indicate that warm Atlantic water replaced cold Arctic water in the western and southeastern Barents Sea (Hald & Vorren 1987; Vorren et al. 1988).

Bulk sediment ^{14}C dates obtained on basal lake sediments from Bjørnøya have been used to date the beginning of the organic production in one of the lakes to between 11,200 ± 500 and 8300 + 1200/−1000 ^{14}C BP (Hyvärinen 1968, 1970; Olsson 1968). However, since the sediments contained large quantities of coal particles derived

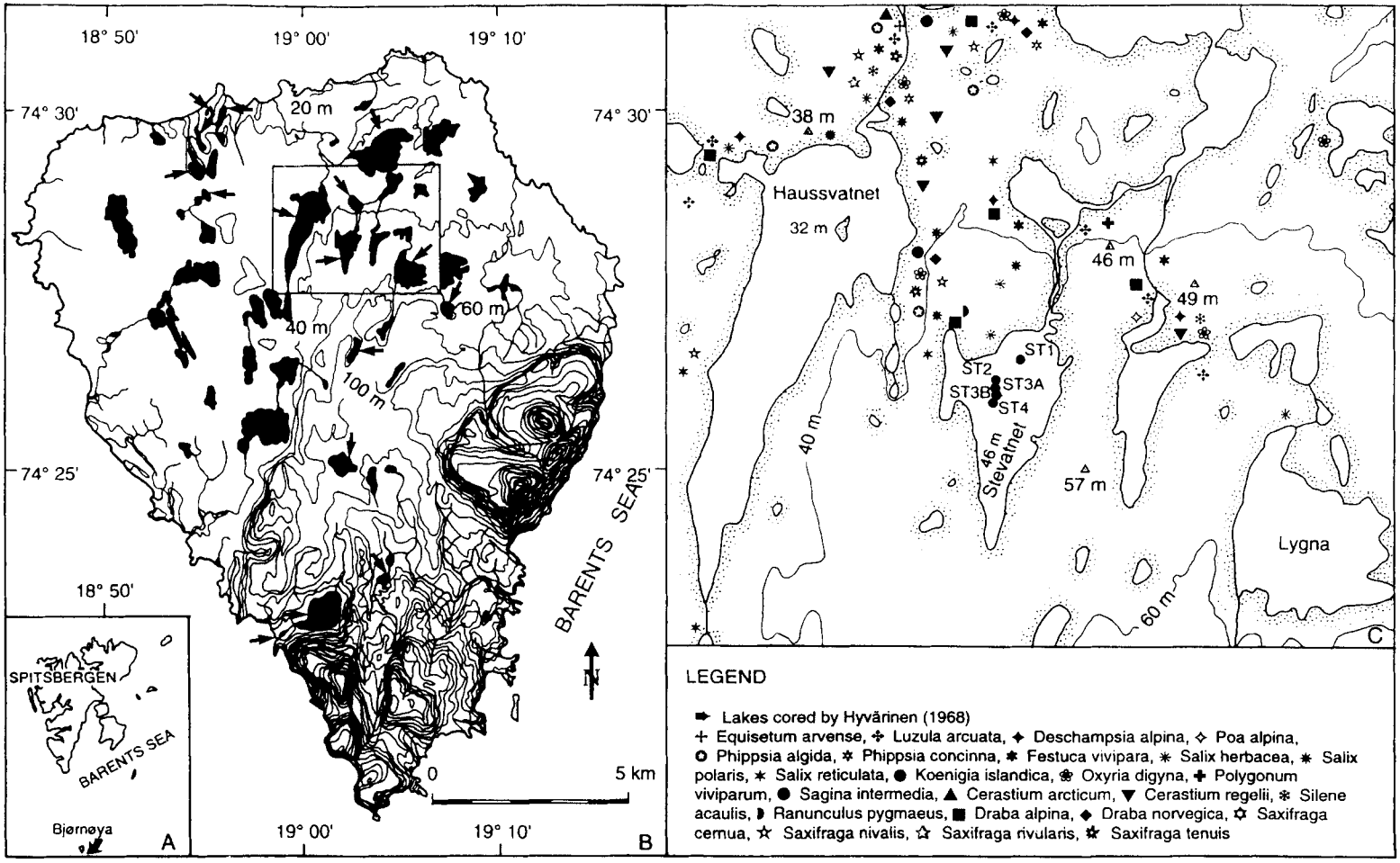

Fig. 1. A. Geographic position of Bjørnøya. B. Topographic map over Bjørnøya. The northern, rather flat part of the island is situated below the 40 m contour line. The mountain areas to the south and southeast reach ca 500 m a.s.l. The lakes cored by Hyvärinen (1968) during the Stockholm University Svalbard Expedition in the years 1965–1966 are marked by arrows. C. Topographic map over the surroundings of Stevatnet. The coring points ST 2–ST 4 are marked with filled circles. The vegetation around the lake is according to Engelskjøn (1986, maps 1–54).

from the bedrock, the reliability of the dates was questioned by Olsson (1968).

The appreciation of the problems associated with the reliability of the original radiocarbon dates from Bjørnøya led to a re-investigation of the sediments of some lakes within the frame of the PONAM project during August 1993. During an earlier Svalbard expedition organised by Stockholm University, Hyvärinen (1968) took sediment cores from 18 lakes situated between 10 and 100 m a.s.l. (Fig. 1B). The Holocene vegetation history was reconstructed on the basis of pollen analysis of three lake sequences and was compared to the development on Svalbard and northern Fennoscandia (Hyvärinen 1968, 1970). Although Horn & Orvin (1928) had described marine terraces/plains of denudation, which they interpreted as younger than the last deglaciation, diatom analyses conducted on lakes at different altitudes did not reveal any marine influence on their sediments (Hyvärinen 1968). During the August 1993 field work we obtained sediment cores from three lakes, Vestre Skinkevatnet, Østre Skinkevatnet and Stevatnet, situated in the northern part of the island. Two of these lakes, Vestre Skinkevatnet and Stevatnet had been cored earlier by Hyvärinen (1968) who described fairly long sediment sequences. The general lithostratigraphy recovered in all three lakes compares well to Hyvärinen's (1968) earlier descriptions.

In this paper we present new results, obtained from geochemical, palynological, entomological, mineral magnetic, plant macrofossil and diatom analyses of sediment cores recovered from Stevatnet. The results, which include new AMS ^{14}C dates, are used to reconstruct the Early Holocene environment on Bjørnøya and are compared to earlier investigations on Bjørnøya and in other Arctic regions.

Geography, climate, bedrock geology and vegetation

The island is surrounded by steep cliffs and has a surface area of 178 km^2. The main geographic units are the fairly flat "northern plain", which extends from southwest to northeast, with altitudes rarely above 40 m a.s.l., and the southern/southeastern part, dominated by hills and mountains that rise up to 500 m a.s.l. Most of the lakes are situated in the "northern plain", which covers a surface area of ca 110 km^2 (Fig. 1B). Many lakes are small, extremely shallow and dry out during summer. Horn & Orvin (1928) observed that the ground thawed to a depth of ca 0.75 m and permafrost reached down to 60–70 m below the surface. However, unfrozen ground below lake bottoms was reported by Fleetwood et al. (1974). Permafrost features such as circles, polygones, nets and stribes are especially common on the limestone terrain.

The maritime arctic climate of Bjørnøya is governed by the Norwegian Current along the western coast and an arctic stream which comes from the east and the north, causing cold air masses to move southwards around the island. Dense fog frequently occurs during the summer months (July: 24 days, August: 22 days) and is a characteristic phenomenon for Bjørnøya. The average yearly temperatures range around ca −1.5°C; the average monthly air temperatures recorded for the time period 1931–1960 range from between −5.7° and −7.2°C for the coldest months January–March and from between +4.5° and +5.0°C for the warmest months, July and August (Steffensen 1969, 1982; Engelskjøn 1986). Since average precipitation does not exceed 400 mm/yr, the high humidity of the ground and the vegetation cover is maintained by the low temperatures and the heavy cloud and fog cover (Engelskjøn 1986).

The bedrock is mainly composed of Devonian, Carboniferous and Permian sandstones, shales, coal seams, conglomerates and fossiliferous limestones (Horn & Orvin 1928; Worsley & Edwards 1976) (Fig. 2A). The oldest and youngest rocks, the dolomites of the Hecla Hoek Formation and the Triassic sandstones and shales, are only found in the mountain areas to the south and southeast.

The strong relationship between vegetation cover and bedrock on Bjørnøya has been described by Engelskjøn (1986), who carried out a detailed survey of the island's plant communities. Although the vegetation can be compared to other areas adjacent to the Barents Sea, several differences exist e.g. between the Spitsbergen and Bjørnøya floras. Compared to Spitsbergen, species adapted to cold and water-logged conditions are more common on Bjørnøya, whereas species demanding higher summer temperatures such as e.g. *Salix glauca*, *Betula nana*, *Dryas octopetala*, *Cassiope tetragona* and *Empetrum hermaphroditum* are absent (Engelskjøn 1986). Most of the island's eutrophic species concentrate on the lime-rich parts, where weathered material

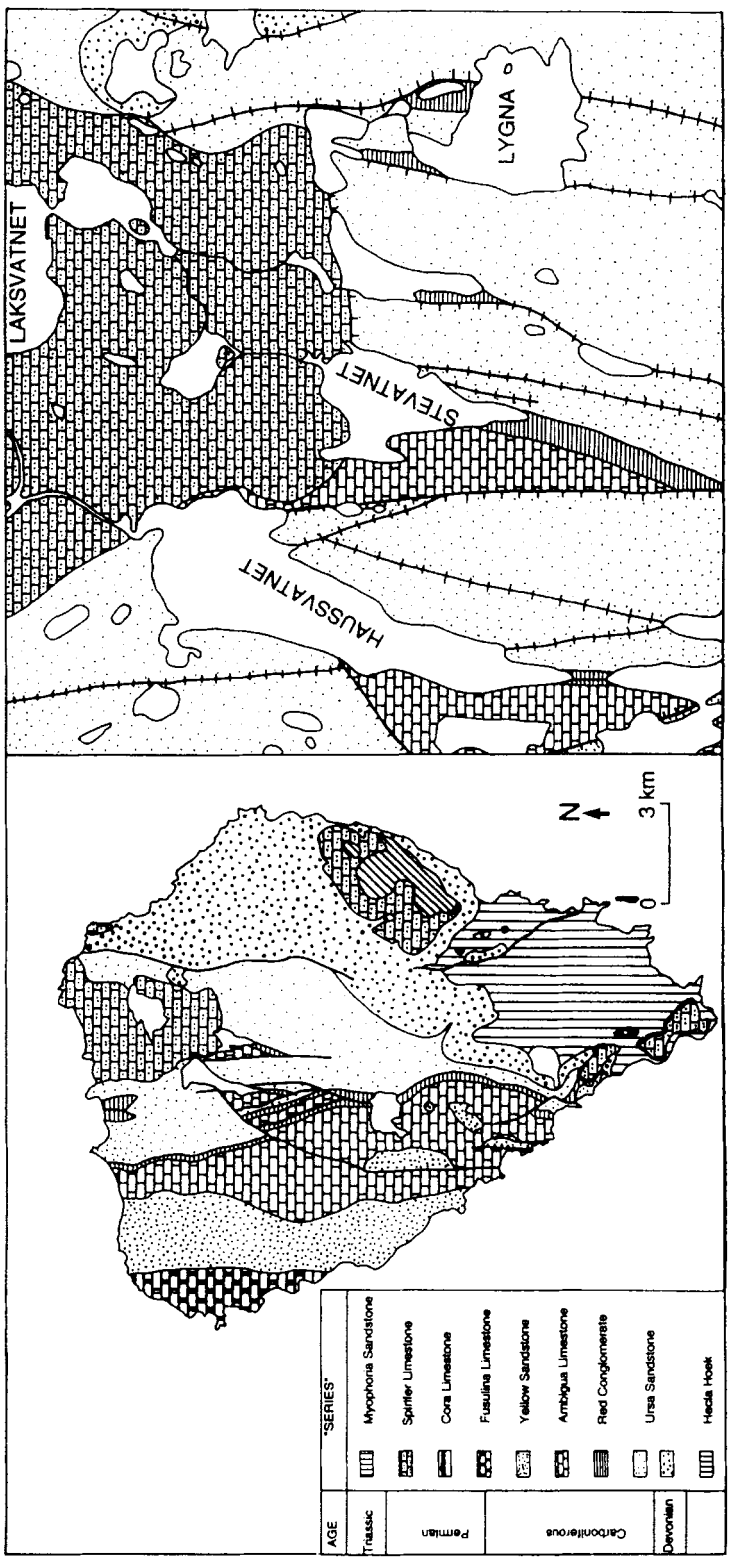

Fig. 2. A. Bedrock geology of Bjørnøya after Horn & Orvin (1928) and Worsley & Edwards (1976). Major fault lines are shown with thick lines. B. Detailed geological map of the surroundings of Stevatnet. Fault lines are indicated by N–S lines with horizontal bars.

from dolomites, limestones and marls yields an alkaline lithosol with a high Ca content (Engelskjøn 1986).

The bedrock-vegetation-relationship is well exemplified in the surroundings of Stevatnet and demonstrated in Figs. 1C and 2B. The soil which developed on the "Spirifer Limestone", a dark grey fossiliferous limestone north of the lake (Horn & Orvin 1928), clearly supports a more extensive vegetation with species such as *Phippsia algida*, *Salix herbacea*, *Salix polaris*, *Salix reticulata*, *Oxyria digyna*, *Sagina intermedia*, *Ranunculus pygmaeus*, *Draba alpina*, *Saxifraga nivalis* and *Saxifraga tenuis* (Engelskjøn 1986). On the western shore of Stevatnet the so-called "Ambigua limestone" series occurs, characterised by massive grey limestones, red and violet mottled limestones and red sandstones (Horn & Orvin 1928). Similar to the eastern shore of the nearby lake Haussvatnet only a sparse vegetation cover with *Salix reticulata* is found (Engelskjøn 1986). The soils which develop on the "Fusulina Limestone" and the "Ambigua Limestone" are alkaline and yield a high content of Ca (Engelskjøn 1986), which explains the more extensive vegetation cover north and east of Stevatnet. The "Red Conglomerate" south of Stevatnet comprises sandstones, calcareous sandstones and conglomerates (Horn & Orvin 1928). It is highly fissile and flakey, and shows a red and yellowish-green colour. The "Ursa Sandstone" east of Stevatnet forms large and coarse blockfields. It is a white to grey massive sandstone with flakes of muscovite and biotite and fairly large amounts of pyrite. The lithosol of the "Ursa sandstone" is slightly acid. Horn & Orvin (1928) and Keilhau (1831) described that the intercalated shaley layers in the "Ursa sandstone" cause it to break up into coarse blockfields or stony polygons. Apart from these stone polygons which support scattered mosses and lichen turfs, the sandstone areas are very poor in vegetation cover (Engelskjøn 1986).

Methods

Fieldwork

Stevatnet is situated at 46 m a.s.l. It has no visible inflow, but drains north into the 12 m lower lake Hellevatnet (Fig. 1C). The core sites (ST 1–ST 4) were concentrated in the western part of the lake, because the water depth in the central part exceeded 6 m and the lake bottom in the eastern part was covered by stones and boulders of the "Ursa Sandstone", which made coring very difficult. Coring was carried out from a specially constructed boat with 1 m long strengthened Russian corers with diameters of 7.5 and 5 cm. The overlap between the cores was ca 20 cm. The lithostratigraphy of the cores was described both in the field and later in the laboratory and revealed a fairly uniform stratigraphy, which made it easy to correlate between different cores, using the transition between layers 7 and 8 as a reference horizon (Fig. 3). The detailed lithostratigraphic description of the four analysed cores (ST 2, 3A, 3B, 4) is based on the field descriptions and given in Tables 1–4.

Mineral magnetic measurements

Routine mineral magnetic measurements were applied to correlate cores and to study the origin of the ferrimagnetic minerals present in the sediments. Detrital magnetic minerals can provide information about the erosion history of lake catchments, while the identification of post-depositional authigenic magnetic minerals may be used to reconstruct sedimentary redox conditions and trophic status.

Samples from all four cores were subsampled into contiguous plastic cubes ($2 \times 2 \times 2$ cm). Cores ST 2 and ST 3A & B were subsampled immediately after collection. However, it was noted that severe oxidation of the cores had taken place during the time that had lapsed between core collection and measurement. Sections of the cores with originally quite distinct FeS stains had become bright red in colour. Core ST 4 was subsampled and measured approximately one year after collection, although the stratigraphy was still in its original form and the FeS colour of the sediment had remained, only with surficial oxidation indicated.

SIRM was induced in a maximum magnetic field of 1 Tesla ($\mu_0 H = 1$ T) with a Redcliff pulse magnetiser, and the remanent magnetisation measured with a Molspin "Minispin" magnetometer. The samples from ST 2 and ST 3A & B were dried at 40°C after measurement to calculate mass specific SI units. In the case of ST 4 magnetic susceptibility (χ) was measured with a Geofyzica Brno "Kappa" bridge and, in addition to the SIRM, a backfield IRM induced at -100 mT was measured to calculate the S-ratio (Stober &

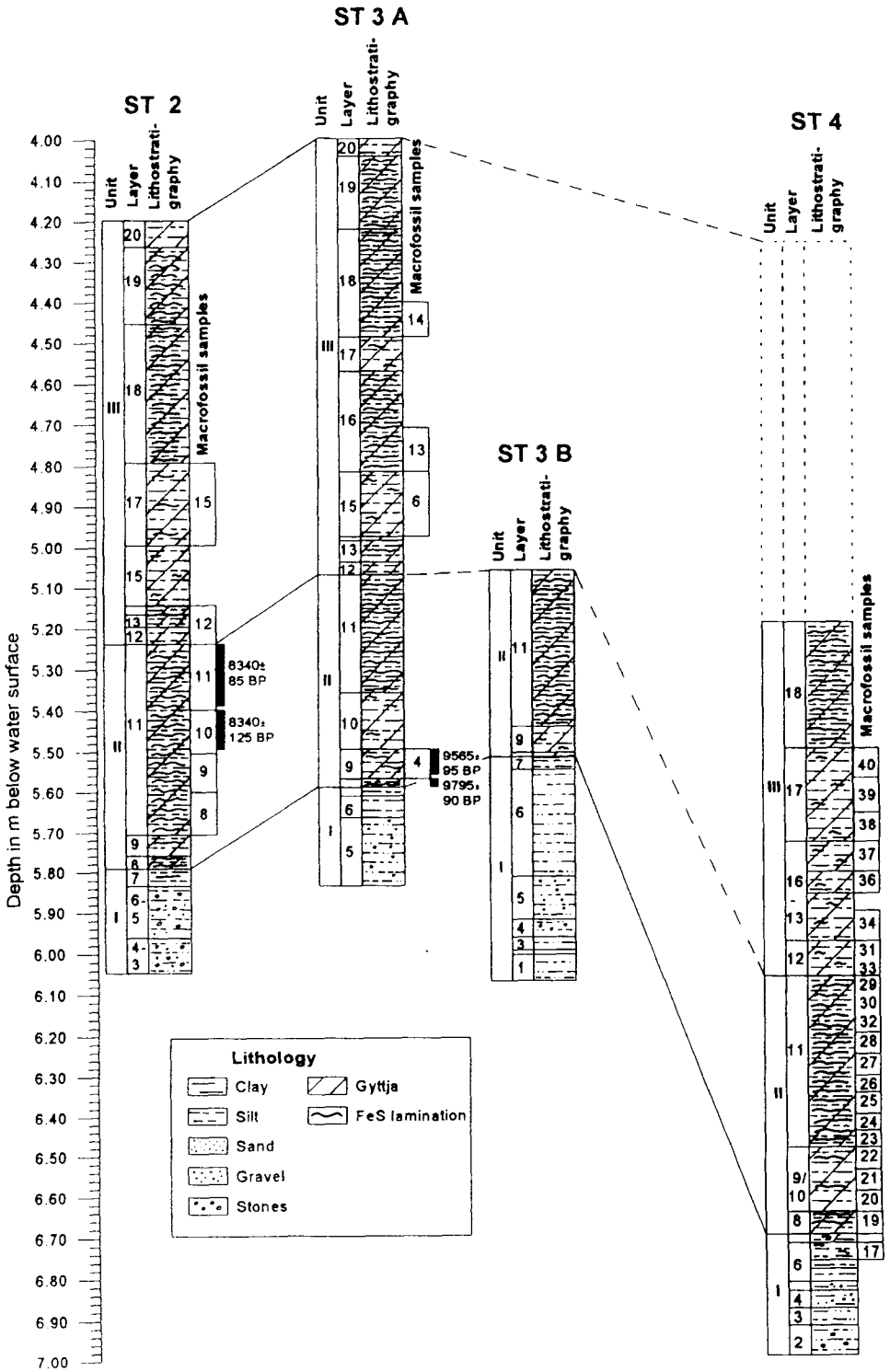

Fig. 3. Lithostratigraphic correlation between cores ST 2, ST 3A, ST 3B and ST 4. The four AMS dates obtained on mosses (ST 3A) and *Salix* leaves (ST 2) are indicated, as well as the samples studied for macrofossils (see Table 6).

Table 1. Lithostratigraphy of core ST 2 at a water depth of 4.20 m. The lithostratigraphic description is based on the field description, where the different gyttja clay layers were mainly distinguished by colour differences.

Unit	Layer	Depth in m	Sediment description
	20	4.20 –4.27	Orange coloured silty gyttja clay, gLB
	19	4.27 –4.46	Alternating layers of light-brown and black (FeS-) coloured silty gyttja clay (ca 20 FeS laminae), moss layer between 4.335–4.345 m, gLB
	18	4.46 –4.80	Black (FeS-) coloured, slightly silty gyttja clay with thin light brown layers (ca 50 FeS laminae), gLB
	17	4.80 –5.00	Light-brown silty gyttja clay with some moss remains and few FeS laminae, gLB
	15	5.00 –5.15	Light-brown silty gyttja clay with some moss remains and some FeS spots, gLB
III	14	5.15 –5.175	Orange-yellow coloured silty gyttja clay with a FeS lamina (0.5 cm thick) at the upper and lower boundary, gLB
	13	5.175–5.21	Light-brown silty gyttja clay, black FeS lamina at 5.20–5.21, g-sLB
	12	5.21 –5.25	Brown silty gyttja clay, gLB
—			
	11	5.25 –5.725	Black (FeS-) coloured clayey gyttja silt with single brown horizons (1 cm thick) and moss remains, g-sLB
II	9	5.725–5.775	Light-brown silty gyttja clay with thin FeS laminae, rich in mosses, gLB
	8	5.775–5.805	Black (FeS-) silty gyttja clay with some moss remains, g-sLB
—			
	7	5.805–5.85	Reddish clayey silt with some FeS laminae, sLB
	6–5	5.85 –5.97	Alternating layers of grey and reddish coloured silty gravelly clay with some small pebbles at 5.94, gLB
I	4–3	5.97 –6.05	Yellow-red-grey coloured gravelly sandy silty clay, compact

Table 2. Lithostratigraphy of core ST 3A at a water depth of 4.00 m. The lithostratigraphic description is based on the field description, where the different gyttja clay layers were mainly distinguished by colour differences.

Unit	Layer	Depth in m	Sediment description
	20	4.00 –4.05	Orange coloured silty gyttja clay, gLB
	19	4.05 –4.23	Alternating layers of black (FeS-) coloured and light-brown silty gyttja clay, gLB
	18	4.23 –4.50	Black (FeS-) coloured silty gyttja clay with thin light-brown layers, gLB
	17	4.50 –4.58	Red-brown silty gyttja clay, some FeS laminae, gLB
III	16	4.58 –4.83	Black (FeS-) coloured silty gyttja clay, higher clay content between 4.65–4.68 m, gLB
	15	4.83 –4.98	Reddish-brown silty gyttja clay, with some moss remains and few FeS laminae, slightly more clayey between 4.96–4.98, gLB
	14	4.98 –4.99	Yellowish silty gyttja clay, black FeS lamina at 4.99, some moss remains, sLB
	13	4.99 –5.04	Reddish-brown silty gyttja clay with thin FeS laminae, some moss remains, gLB
	12	5.04 –5.085	Yellowish silty gyttja clay, g-sLB
—			
	11	5.085–5.37	Black (FeS-) coloured, silty gyttja clay with few brown coloured laminae, some moss remains, sLB
	10	5.37 –5.50	Brown-yellowish silty gyttja clay with some FeS laminae (0.5–2 cm thick), some moss remains, sLB
II	9	5.50 –5.58	Reddish-brown silty gyttja clay, faintly FeS laminated, rich in mosses, sLB
	8	5.58 –5.605	Black (FeS-) silty gyttja clay, some moss remains, g-sLB
—			
	7	5.605–5.625	Red-brown silty clay, very sLB
I	6	5.625–5.67	Grey-reddish silty clay, sLB
	5	5.67 –5.84	Grey silty sandy gravelly clay

Thompson 1979). These samples were not air dried and are currently under further investigation. Certain sediment sections of ST 4 were selected for concentration of the magnetic minerals in accordance with the methods of Snowball & Thompson (1990). Samples were freeze-dried to prevent oxidation of possible magnetic iron sulphides and the magnetic fractions were stored in acetone. The magnetic extracts were dispersed in epoxy resin and the magnetic hysteresis properties of the ferrimagnetic fraction measured with a PMC AGFM-2900-2 magnetometer. The variation of magnetisation with temperature was investigated with the aid of a horizontal force translation balance at the University of Edinburgh.

X-ray diffraction analysis (XRD) was used to identify the magnetic minerals recovered in the magnetic concentrates. Powder preparations were prepared of magnetic extracts and X-ray scanned over the region 15–55° 2θ using a Philips diffractometer with Cu K_α-radiation.

Grain size and geochemistry

The grain-size distribution of samples from cores ST 3A & B was performed by sieving pre-weighed samples through a 63 μm sieve. The coarse fractions were further sieved, dried and weighed, while the fine fractions were analysed on a Sedigraph 5000 ET (Micromeritics) after deflocculation in $Na_4P_2O_7$. The results were recalculated to bulk samples.

Total carbon content was determined on cores ST 3A & B by stepped heating of the samples in oxygen in a Leco furnace, which measures the CO_2 evolved by IR detection (Leco multiphase carbon analyser RC-412). Besides organic material, the sediments also contain a minerogenic carbon phase (coal), which is thermally stable up to temperatures of 450–500°. To separate organic carbon (C_{org}) from bedrock derived carbon present as coal (C_{min}) the amount of minerogenic carbon was estimated after oxidation of separate samples with H_2O_2 and HNO_3, which preferentially oxidises the organic matter. Both carbon phases are reported as weight % C of the dry matter.

The total sulphur content was determined on subsamples from cores ST 3A, B & ST 4 after digestion of the samples at 450°C in a mixture of KNO_3 and $NaNO_3$ (50/50 molar %) followed by dissolution in a reagent solution of $KNO_3/NaNO_3$ in HCl (McQuaker & Fung 1975). The sulphur content was then measured gravimetrically after hot precipitation of SO_4^{2-} as $BaSO_4$.

Macro- and microfossil analysis

For macrofossil analyses, 5–15 cm thick samples from ST 2, ST 3A and ST 4 were pre-treated with 10% NaOH and sieved through a 0.25 mm mesh. The macrofossils were sorted out under a binocular microscope. Identifications were carried out by comparisons with modern reference material. The reconstruction of the thermal cli-

Table 3. Lithostratigraphy of core ST 3B at a water depth of 4.00 m. The lithostratigraphic description is based on the field description, where the different gyttja clay layers were mainly distinguished by colour differences.

Unit	Layer	Depth in m	Sediment description
	11	5.07 –5.45	Black (FeS-) coloured silty gyttja clay with brown-yellowish layers and some moss remains, gLB
II	9	5.45 –5.51	Reddish-brown silty gyttja clay, rich in mosses, some FeS laminae, sLB
	8	5.51 –5.52	Black (FeS-) silty gyttja clay, fairly rich in mosses, g-sLB
—			
	7	5.52 –5.56	Reddish-brown and greenish silty clay, FeS laminae in the upper part, sLB
	6	5.56 –5.65	Reddish-grey sandy silty clay, very compact, sLB
	5	5.65 –5.82	Grey silty sandy gravelly clay with small angular stones (3 cm Ø), clay layer between 5.715–5.735, gLB
I	4	5.82 –5.935	Yellow-grey silty sandy gravel, with silty clay layers, gLB
	3	5.935–5.97	Reddish, sandy silty clay, compact, gLB
	2	5.97 –6.00	Yellow-grey sandy silty gravelly clay, compact
	1	6.00 –6.07	Reddish to red-brown, sandy silty clay, compact

mate was made by using the Mutual Climatic Range method (MCR) on fossil *Coleoptera*. This method is based on the present geographical ranges of the species in relation to modern temperature (Atkinson et al. 1986). The palaeotemperatures were reconstructed by use of the mutual intersection of the climatic ranges of selected stenothermic species in the fossil record. The MCR method reconstructs mean July (warmest month) temperature (TMAX) and mean January (coldest month) temperature (TMIN). One of the great advantages of the MCR method is that it is possible to test its accuracy on modern *Coleoptera* assemblages in relation to climate. Such studies have shown the need of a calibration of the MCR results to obtain the most probable palaeotemperature (Atkinson et al. 1987). This calibration is carried out by using the correction equations:

$$TMAX_{(corrected)} = 1.066\ TMAX_{(median)} + 0.0142 \times \text{No. of species} \times -2.96$$

$$TMIN_{(corrected)} = 1.416\ TMIN_{(median)} + 1.904$$

The precision of the most probable palaeotemperature is ca ± 2°C for TMAX and ca ± 5°C for TMIN.

In ST 3A subsamples for pollen (including spores, *Pediastrum* and *Botryococcus*) were spaced every 5 cm in the upper layers (layers 10–15) and every 2 cm in the basal layers (layers 6–9). The samples (2 cm^3) were treated with $ZnCl_2$ and prepared according to conventional procedures. Tablets with *Lycopodium* spores were added to the pollen samples to determine concentration values. The group of *Betula* pollen includes both tree and dwarf birch.

Subsamples for diatoms in core ST 3A were prepared in accordance with the methods described by Battarbee (1986).

AMS ^{14}C measurements

To obtain datable material for AMS measurements subsamples from cores ST 2, ST 3A and ST 4 were sieved through a 0.5 mm mesh and the macrofossils recovered were determined under a stereomicroscope. Intact leaves of *Salix* species were immediately dried on aluminium foil (at 50°C over night), stored in sterilised glass bottles and sent to the Tandem Laboratory in Uppsala. A full pre-treatment (including 1% HCl, 6 hrs at 80°C and 0.5% NaOH, 1 hr at 60°C) was applied to the *Salix* samples. The moss remains were submitted in distilled water and pretreated with 1% HCl (6 hrs at 80°C).

Table 4. Lithostratigraphy of core ST 4 at a water depth of 4.25 m. The lithostratigraphic description is based on the field description, where the different gyttja clay layers were mainly distinguished by colour differences.

Unit	Layer	Depth in m	Sediment description
	18	5.20 –5.50	Alternating layers of black and beige-brown coloured silty gyttja clay with moss remains, gLB
	17	5.50 –5.74	Slightly FeS coloured silty gyttja clay with moss remains; more FeS laminae between 5.50–5.60, 5.60–5.64, 5.68–5.70, gLB
	16	5.74 –5.81	Light-brown silty gyttja clay with moss remains and few FeS spots, gLB
III	15/14	5.81 –5.865	Light-brown silty gyttja clay, at 5.845–5.85 and 5.86–5.865 yellow coloured layers, sLB
	13	5.865–5.98	Light brown silty gyttja clay, FeS laminations only between 5.94–5.95, otherwise FeS spots, moss remains, gLB
	12	5.98 –6.07	Reddish-brown silty gyttja clay, mosses, FeS spots, gLB
—			
	11	6.07 –6.49	Alternating layers of black (1–3 cm) and brown-reddish (0.5 cm) silty gyttja clay, gLB
II	9/10	6.49 –6.65	Alternating layers of black, greenish, brown-reddish silty gyttja clay, pebble at 6.565, gLB
	8	6.65 –6.70	Black moss-rich silty gyttja clay, gLB
—			
	7	6.70 –6.73	Reddish-brown silty gyttja clay, FeS spots and laminae, moss remains, gLB
	6c	6.73 –6.77	Reddish-brown clayey silt, few FeS spots, g-sLB
	6b	6.77 –6.785	Greenish clayey silt separated by a brown-reddish clay layer (3 mm), sLB
I	6a	6.785–6.82	Reddish silty clay, very sharp LB
	5	6.82 –6.84	Greenish sandy gravelly clay, unregular LB
	4	6.84 –6.88	Reddish clayey sandy gravel, g-sLB
	3	6.88 –6.93	Reddish-brown sandy silty clay, pebbles, sLB
	2	6.93 –7.00	Greenish, yellow, reddish laminated sandy silty clay, pebbles, soft

Results

Lithostratigraphy, grain size and geochemistry

The lithostratigraphy of the sediments was described in the field where the fresh cores all showed very distinct black FeS stains and horizons, which (with the exception of core ST 4) were found to have disappeared (due to oxidation) when the cores were unwrapped in the laboratory. The lithostratigraphy presented in Tables 1–4 mainly follows the field description, but has been verified in the laboratory. The distinction in different sediment layers (1–20) is based on sediment colour, grain size and organic content. However, because postdepositional chemical reactions are responsible for the colour differences of the sediment column, the lithostratigraphic sequence was divided into three units. Unit I comprises layers 1–7, unit II layers 8–11 and unit III layers 12–20.

The lowermost minerogenic sediment layers of unit I were recovered in all four cores, but attain a maximum thickness of 55 cm in ST 3B only. In this core the compact reddish-brown and yellow-grey sediments between 6.07–5.935 m (layers 1–3) show a gradual transition from sandy silty clay to sandy gravelly silty clay and sandy silty clay (Fig. 3, Table 3). Between 5.935–5.82 m (layers 4–5), the sediments are composed of loose sandy clayey gravel and sandy gravelly clay with small pebbles. A reddish-grey sandy silty clay (layer 6) and a silty clay with some FeS stains (layer 7) follow with sharp lower boundaries (Fig. 3, Tables 1–4). The water content is constant (ca 20–30%) and reflects the dominance of the silt and sand fractions (>55%) in these bottom layers (Fig. 4). In the uppermost part of unit I, the water content increases slightly to 35%, the sand fraction decreases to 0% and the silt and clay fractions dominate the grain size distribution. The total carbon content (C_{tot}) varies between 0.3 and 3.3%. Coal particles (C_{min}) derived from the bedrock are the dominant carbon source with between 0.4 and 3.1%. Organic carbon (C_{org}) contributes between 0.2 and 0.8%. The sulphur content is stable below 0.1% (Fig. 4).

The transition from unit I to unit II is characterised by a drastic change in colour and lithology from reddish-brown silty clay to black silty gyttja clay (Fig. 3). In cores ST 2, 3A and 3B, the silty gyttja clays in the lower part of unit II are light-brown, reddish-brown and brown-yellowish, whereas the corresponding layers in ST 4 show alternating black, greenish and brown-reddish laminae. The silty gyttja clay in the upper part of unit II is characterised in all four cores by alternating black and brown-reddish laminae (Fig. 3, Table 1–4). The lower boundaries of layers 9 and 10 appear sharp. Layer 10 is only present in cores ST 3A and ST 4 and seems to be missing in ST 2 and ST 3B. The water content increases rapidly from 40% to 60% at the transition from unit I to unit II and attains 80% in the upper part of unit II. The grain size distribution is dominated by clay and silt, which attain ca 50% each, apart from two excursions at 5.30–5.22 and at 5.10 m, where the sand fraction increases to 10% and 5% respectively (Fig. 4). The content in C_{tot} increases from 1.6% at the transition unit I/II to a maximum of 4.3% in the upper part of unit II. This increase is entirely attributable to organic matter. Parallel with the increase in C_{org}, the sulphur values rise from 0.2% to 1.8% and remain constant between 0.8 and 1.3% in unit II. When comparing the curves for organic carbon and sulphur, it becomes obvious that high carbon values coincide with peaks in the sulphur content.

The upper half of the Stevatnet sequence, unit III (layers 12–20) comprises silty gyttja clays with colours varying from yellowish, light-brown, reddish-brown to black. The water content decreases slightly to between 65–70%, but varies, especially in the upper part of unit III between 55–75%. The grain size distribution displays a dominance of the silt (ca 40%) and clay 50–60% fraction. In the upper part of unit III, at 4.29 m, the clay fraction (<2 μ) decreases to 20% and the silt fraction (<60 μ) increases to 70%. The total carbon content displays in general a slightly decreasing trend from 3.2% in the lower part of unit III to 2.5% in the top. C_{org} remains the major fraction of the total carbon content, whereas minerogenic carbon is nearly constant at ca 0.4–0.6%. The sulphur values show a similar gradual decrease from 0.9% to less than 0.2%. Higher sulphur values at 5.02 m (1.1%), 4.94 m (1.2%) and between 4.10–4.20 m (0.4%) coincide with higher C_{org} values.

Mineral magnetics

A critical prerequisite for the correct environmental interpretation of mineral magnetic investigations is the analysis of fresh samples (in this case prior to oxidation). The results obtained from core ST 4 are presented first as it was noted

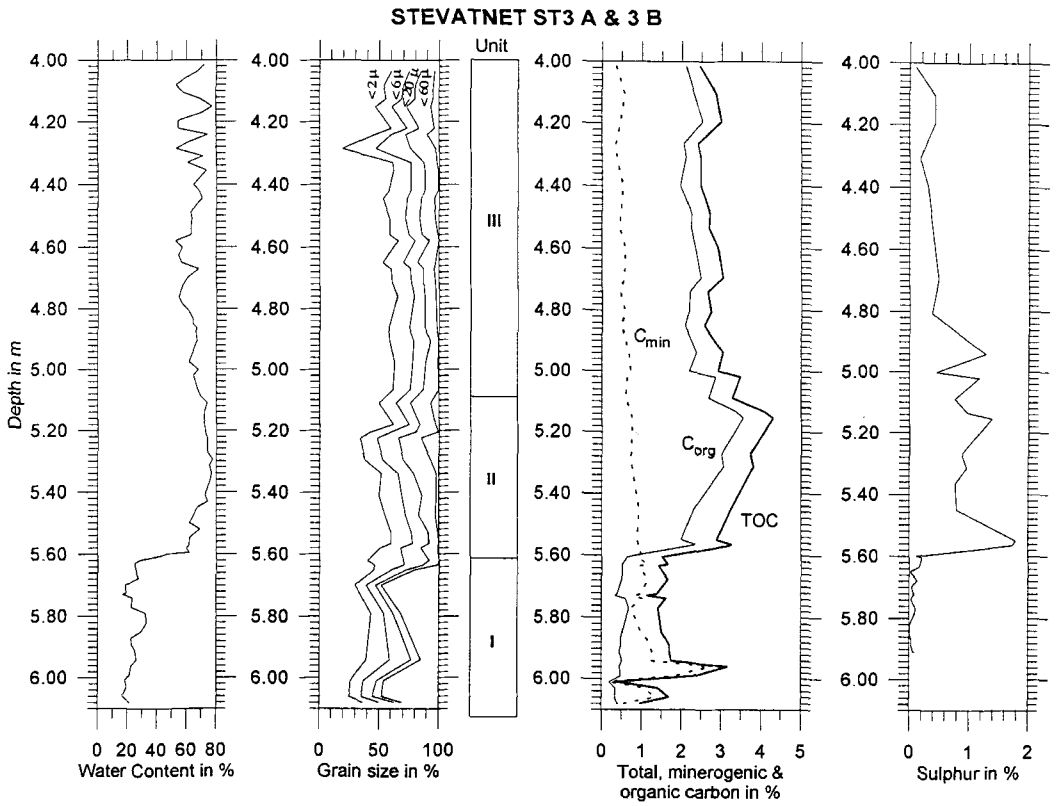

Fig. 4. Water content, grain size, carbon and sulphur content of cores ST 3A and 3B. The lithostratigraphy and the analyses below 5.62 m are interpolated from core ST 3B.

that the well-wrapped sediments had not oxidised during storage and that the original FeS stratigraphy remained intact (see above).

Fig. 5 displays the mineral magnetic properties of bulk samples taken from core ST 4. χ and SIRM are generally low in unit I, between a depth of 7.00 and 6.68 m, and indicate a low concentration of magnetic minerals in the minerogenic sediments, while the high S-ratio indicates that antiferrimagnetic minerals (e.g. goethite/haematite) dominate the mineral magnetic properties. A distinct change occurs in the magnetic properties at the transition from unit I to unit II, at 6.68 m, and the concentration of ferrimagnetic minerals (indicated by χ and SIRM) increases dramatically. The S-ratio decreases to −0.8 and indicates that a "soft" magnetic mineral (e.g. magnetite/greigite) dominates the mineral magnetic assemblage up to the top of the core. Apart from the lowermost sample at 6.68 m, only insignificant fluctuations occur in the magnetic parameters up to a depth of 5.80 m. In unit II, between 5.80 and 5.50 m the concentration parameters and the S-ratio fluctuate, although they return to stable values in unit III, between 5.50 and 5.23 m. The linear relationship between SIRM and χ in the sediment above 6.68 m (Fig. 6) indicates that only one ferrimagnetic mineral makes a significant contribution to the mineral magnetic assemblages in the sediments above 6.68 m.

The thermomagnetic behaviour of a magnetic concentrate from a sediment depth of 6.68 m (with high ferrimagnetic concentration) is shown in Fig. 7A. The almost completely irreversible loss of magnetization between 300 and 400°C is typical of ferrimagnetic greigite when heated in air (Snowball & Thompson 1990). The sharp rise in magnetisation on heating at 150°C is explained by the additional formation of greigite in the

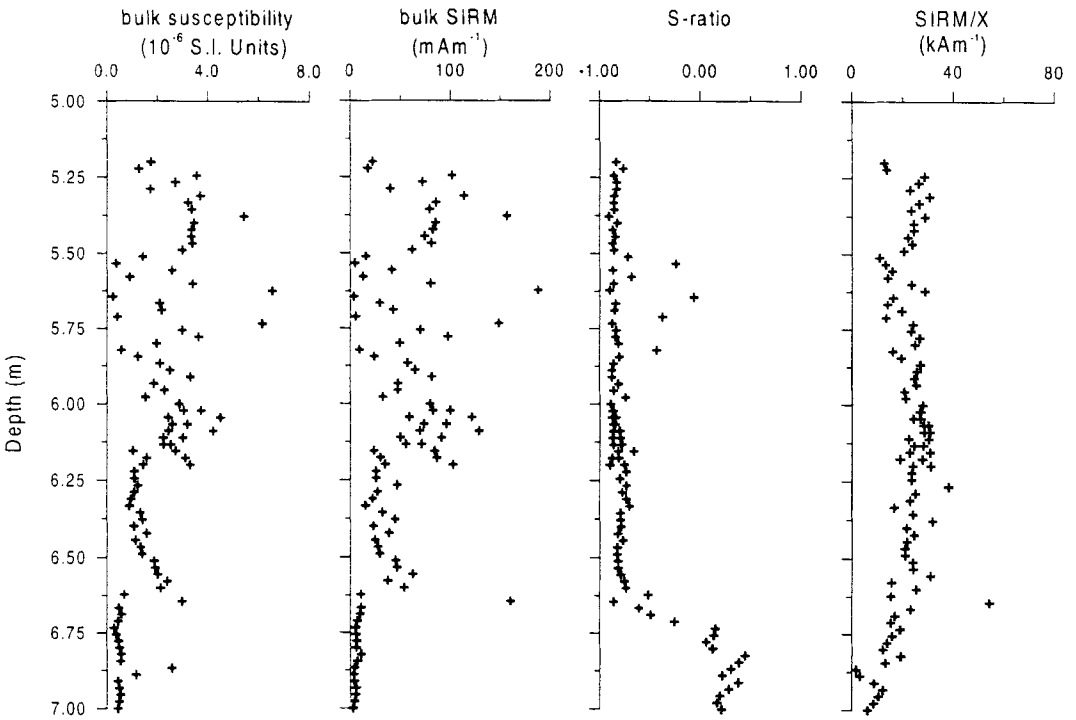

Fig. 5. Mineral magnetic properties of core ST 4.

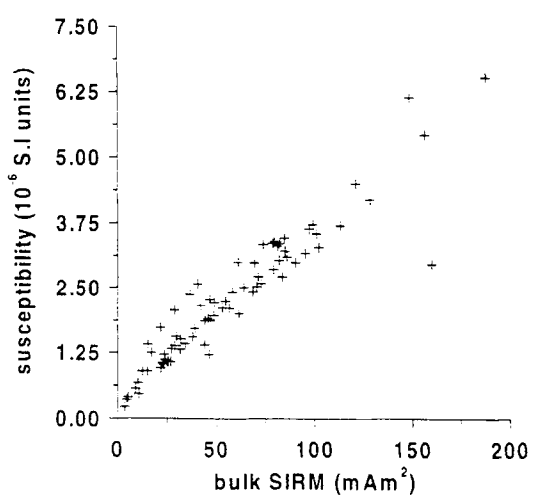

Fig. 6. SIRM vs magnetic susceptibility for the sediments above a depth of 6.68 m in core ST 4. The linear relationship demonstrates that one mineral contributes to the magnetic assemblage.

sample (Snowball 1991), produced from a phase transformation of unidentified iron sulphides associated with the ferrimagnetic concentrate. The curve shown is typical of those obtained from magnetic concentrates of sediments above 6.68 m and they demonstrate that the magnetic properties are dominated by greigite. The X-ray diffraction analysis of the magnetic concentrate confirms the identification of the ferrimagnetic phase as greigite (Fig. 7B). A magnetic hysteresis curve, representative of the magnetic concentrates is shown in Fig. 7C. The very open central section is typical of natural greigite samples (Snowball 1991) and the high M_{RS}/M_S ratio (0.56) and low $(B_O)_{CR}/(B_O)_C$ ratio (1.3) indicate that the greigite is of a single-domain magnetic grain size. Greigite of variable morphology (needles, plates, cubes etc.) formed by authigenesis at low temperatures and pressures in sediments has normally been found to exhibit single-domain magnetic behaviour.

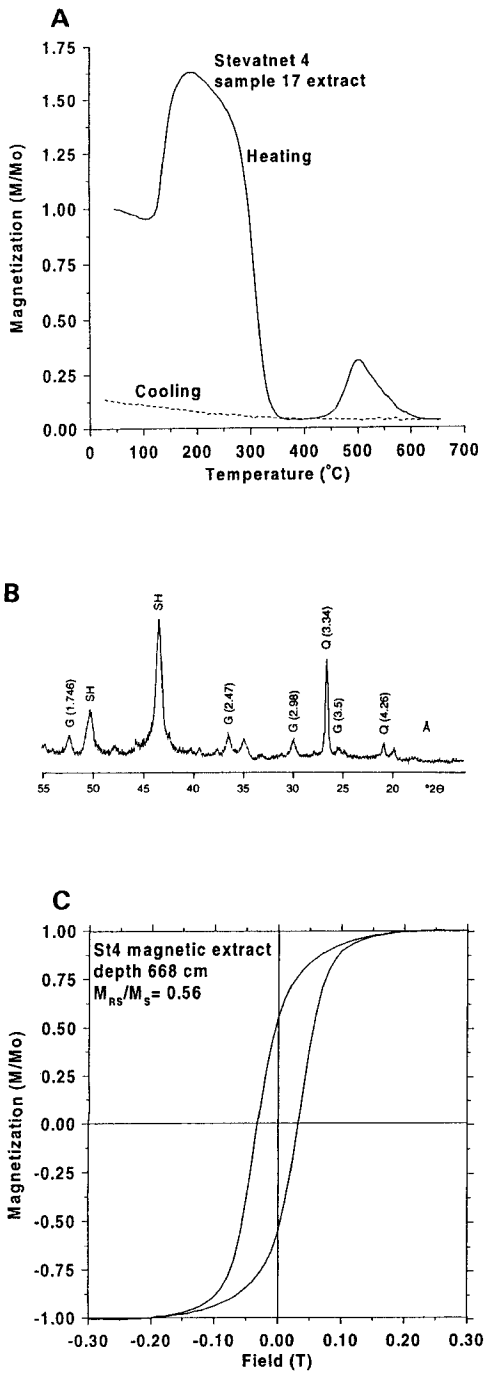

Fig. 7. A. Typical thermomagnetic curve of a magnetic concentrate. The curve indicates the presence of greigite and the absence of magnetite. B. XRD pattern of magnetic concentrate. Greigite is the only ferrimagnetic mineral present. G = greigite, Q = quartz, SH = sample holder. CuKα radiation was applied. C. The hysteresis loop of a magnetic concentrate. The loop is characteristic of single-domain greigite grains.

The more scattered nature of the SIRM and S-ratio curves in unit III of core ST 4, between 5.80 and 5.50 m, is linked to the observed stratigraphy and is caused by the precipitation of greigite on the surfaces of relatively large moss remains. The discovery that greigite is responsible for the mineral magnetic characteristics of the sediment that lies above 6.68 m in core ST 4 aids in the interpretation of the SIRM measurements carried out on the other cores. Fig. 8 displays SIRM values for all four cores. Greigite is responsible for high values of SIRM above the lowermost minerogenic sediments. Although it is still possible to delimit the different stratigraphic layers in ST 2, ST 3A and 3B, based upon the mineral magnetic measurements, only the magnetic properties of ST 4 can be considered representative of the fresh sediment. The postdepositional authigenic formation of ferrimagnetic greigite prevents the interpretation of the mineral magnetic results in terms of catchment erosion. However, specific geochemical conditions are required to promote greigite formation. Greigite is a precursor to pyrite and may be preserved in sediment sequences when pyrite formation is limited by sulphur availability (Berner 1981). The occurrence of greigite in the Early Holocene sediments indicates that anoxic conditions prevailed in the deeper regions of the basin following the onset of the deposition of organic material. The C_{org}/S_t ratio is approximately 4 in unit II of ST 3A (between 5.6 and 5.0 m), but increases to ca 7 above 5.0 m and indicates that sulphur availability became a limiting factor in greigite authigenesis. The lower SIRM values in unit III of core ST 3A are due to the absence of greigite authigenesis, which indicates that the sedimentary environment altered between a depth of 5.0 and 4.8 m in core ST 3A.

Microfossil analysis (pollen, spores, algae)

Pollen. – The pollen diagram (Fig. 9) covers the lower part of core ST 3A. The total pollen sum ranges between 54–130 pollen/sample in the bottom part, and increases to between 112–418 pollen/sample further up in the sequence.

SPZ 1: *Artemisia-Oxyria/Rumex-Betula* zone (5.62–5.52). This pollen zone, which comprises the two lowermost samples (below and above the transition from unit I to unit II), is characterised by approximately equal proportions of herb and *Betula* pollen. *Artemisia* values attain 20% in the

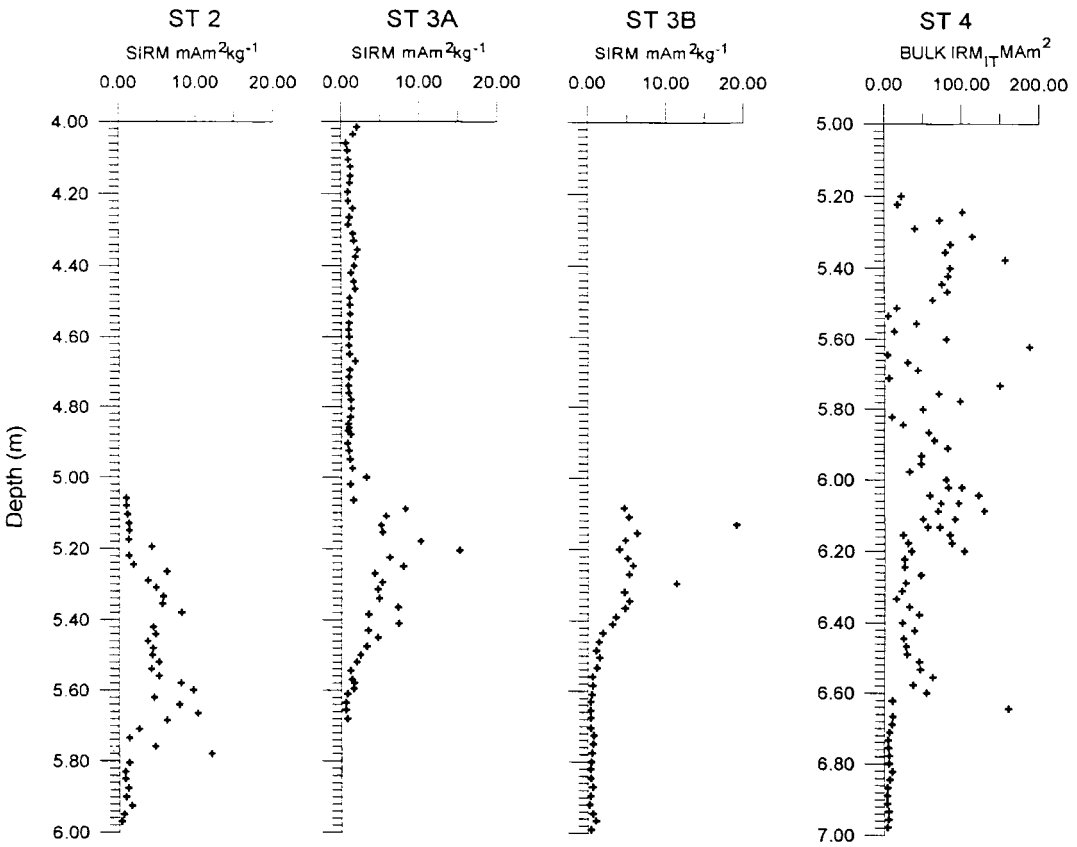

Fig. 8. The SIRM of ST 2, ST 3A & B and ST 4. Greigite is responsible for the high values of SIRM in all of the cores.

bottom sample, but decrease to 10% in the upper sample, whereas *Oxyria/Rumex* frequencies increase to 30%, but show a slow decrease in the upper part of this zone (10%).

SPZ 2: *Oxyria/Rumex-Betula-Pinus*-zone (5.52–4.95 m). During this pollen zone, herb pollen values decrease gradually from 45 to 10%, while frequencies of tree pollen increase from 55 to 90%. *Oxyria/Rumex* values decrease gradually from 30 to 5%. *Salix* and *Artemisia* pollen frequencies remain at ca 5%, but decrease in the upper part to ca 2.5%. *Juniperus* values increase slightly during the uppermost 20 cm, but do not attain more than 5%.

The lowermost local pollen zone SPZ 1 compares well with Hyvärinen's (1968, 1970) zone I, where he describes abundant non-arboreal pollen (NAP) with a dominance of *Betula* among the tree pollen. The second local pollen zone SPZ 2 may be compared with zone IIa in Hyvärinen's (1968, 1970) diagrams, where lower NAP values and a rise in *Alnus* are reported. There is, however, a major difference between our diagram and the diagrams presented by Hyvärinen (1968, 1970): *Pinus* pollen values attain rarely more than 20% in our diagrams, but increase in Hyvärinen's (1968, 1970) zone II to more than 50%. This might be explained by the fact that we could have lost a major part of the pine pollen during the pollen preparation, where we applied a $ZnCl_2$ treatment to separate the pollen grains.

Our pollen spectrum is clearly dominated by long-distance transported pollen grains. All tree pollen (*Betula*, *Pinus*, *Alnus*) and most of the non-arboreal pollen (*Artemisia*, Chenopodiaceae, *Filipendula*, *Urtica*, *Juniperus*, Caryophyllaceae) must be regarded as exotic. *Salix*, Gramineae, Cyperaceae, *Oxyria/Rumex*, Rosaceae might represent a mixture of local and long-distance transported pollen. Ranunculaceae,

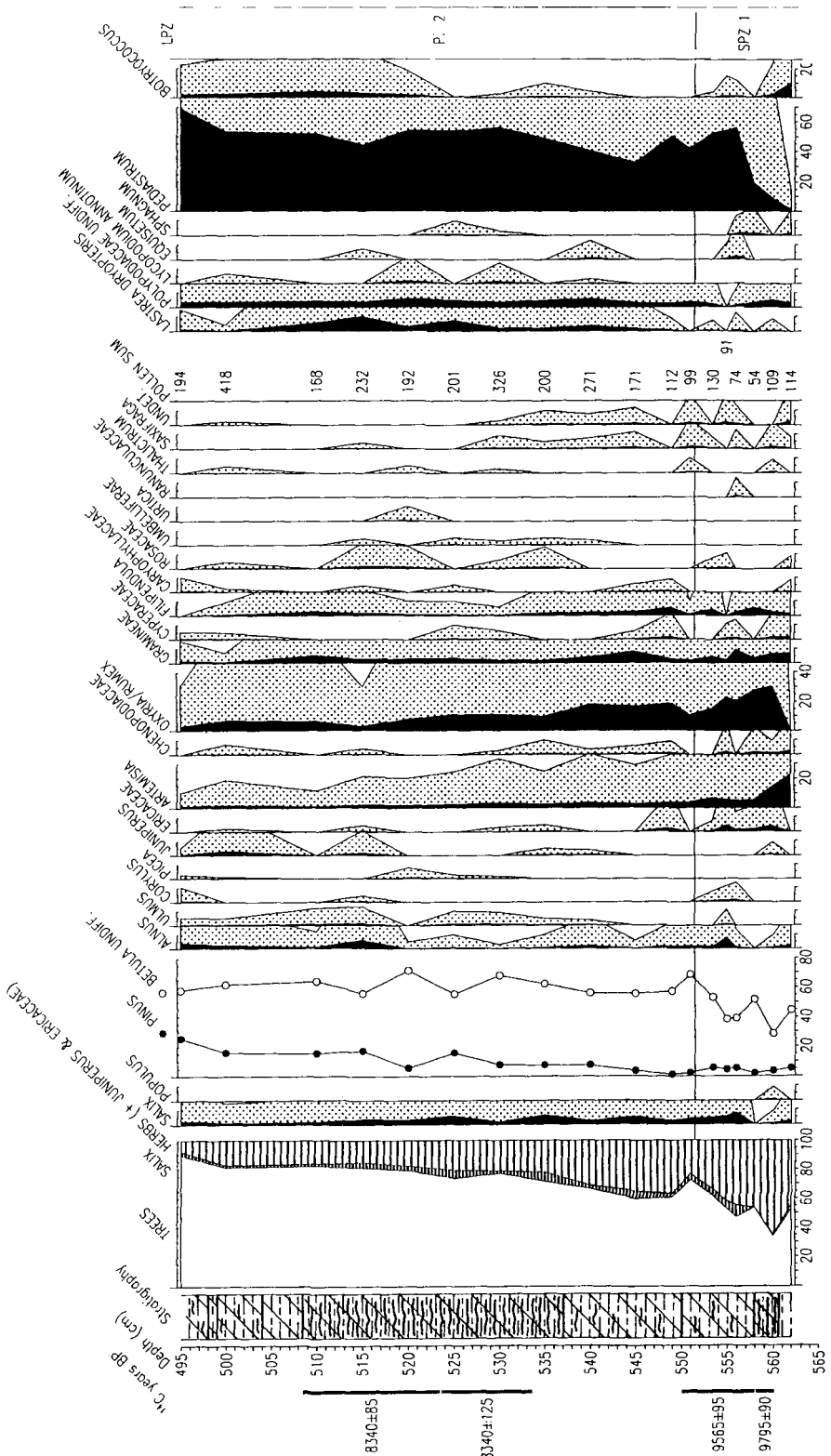

Fig. 9. Pollen, spore and algae percentage diagram of core ST 3A.

Ericaceae and *Saxifraga* which occur in the recent flora (Engelskjøn 1986) may have grown on the island. The dominance of long-distance transported tree pollen in the pollen spectrum is a typical feature in Holocene pollen spectra from e.g. Spitsbergen (Hyvärinen 1970) or northern Fennoscandia (e.g. Hjelmroos & Franzén 1994). Possible sources include areas adjacent to the Barents Sea but may be as far south as South Europe/North Africa (Hjelmroos & Franzén 1994).

Spores and algae. – Spores of Polypodiaceae (undiff.) are present throughout the whole sequence with ca 5%. *Lastrea dryopteris* appears from ca 5.51 m upwards (Fig. 9). It attains values of 10% at 5.15 m, but decreases below 5% between 4.99–4.95 m. All spores are regarded as long transported. *Pediastrum* values increase very rapidly from less than 5% at 5.62 m to 10% at 5.60 m and to 50% at 5.56 m. In the upper part of the sequence *Pediastrum* values are around 50–70%. *Botryococcus* decreases from 10% at 5.62 m to less than 5% at 5.55 m. It is not present between 5.52–5.40 m, but increases again from 5.40 m upwards.

Diatoms. – Diatoms are extremely rare in most of the analysed samples of core ST 3A (Table 5). In unit I and in the lowermost part of unit II only few, quite heavily corroded diatoms were found. However, higher up in unit II, the preservation was slightly better. The diatom assemblage is dominated by *Brachysira* species and includes *Stauroneis anceps*, *Fragilaria pinnata*, *Amphora libyca*, *Amphora* cf. *veneta*, which indicate freshwater conditions and a probably higher pH than that found in the top sample. Between 5.50–4.50 m (units II and III) the diatoms are again very badly preserved. Although the species recovered at 4.50 m are also poorly preserved and dissolved, robust forms, such as *Fragilaria pinnata*, *Frustulia* sp. and *Pinnularia* can be recognised. *Fragilaria pinnata* is fairly common in soft waters. Only in the top sediment at 4.00 m, where *Fragilaria virescens* var. *exiguam* becomes the dominating form, are the diatoms abundant and well preserved. All the species recorded at 4.50 m are benthic forms and indicative of slightly acid (possibly around pH 5–6) and shallow waters. Shallow water could explain the absence of centric forms.

Macrofossil analysis

Macroscopic remains of plants and animals were sorted out from cores ST 2, ST 3A and ST 4 (Fig. 3). The results of the identification are shown in Table 6. The following remarks on the vegetational and faunal record is based on the modern biology and geographical distribution of the mentioned taxa (Palm 1948; Rønning 1979; Engelskjøn 1986; Fitter & Manuel 1986; Hultén & Fries 1986; Nilsson & Persson 1989; Mossberg et al. 1992).

In general, mosses and midges dominate the fossil assemblages and are present from the lowermost analysed samples in unit I to the uppermost sample in unit III. Mosses are especially frequent in the lower part of unit II. Leaf fragments of dwarf willows such as *Salix reticulata*, *S. herbaceae* and *S. polaris* are recorded in units II and III (Fig. 3 & Table 6). These species are today dominant or characteristic in plant communities on well-

Table 5. Diatom taxa recorded in core ST 3A.

Depth (m)	Unit	Diatom taxa (listed according to their frequency)
4.00	III	*Fragilaria virescens* var *exigua*, *Fragilaria construens* var *venter*, *Navicula cocconeiformis*, *Cymbella gaumanii*, *Achnanthes flexella*, *Navicula digitulus*, *Pinularia* sp., *Frustulina rhomboides* var *saxonica*, *Achnanthes scotica*
4.50	III	*Fragilaria pinnata*, *Frustulia* sp., *Pinnularia* sp.
5.00	III	few/no diatoms
5.37	II	few/no diatoms
5.54	II	*Stauroneis anceps*, *Fragilaria pinnata*, *Amphora libyca*, *Amphora* cf. *veneta*, *Brachysira* sp.
5.59	II	diatoms are extremely rare
5.61	I	diatoms are extremely rare
5.62	I	diatoms are extremely rare
5.66	I	diatoms are extremely rare

drained and exposed ground in the inland of Bjørnøya. In two samples from the upper part of unit II (layer 11), rather corroded leaf remains of *Dryas* sp. were found. This plant grows on calcareous soils in Spitsbergen and Scandinavia, but is not found on Bjørnøya. This species is probably absent because it requires higher summer temperatures than those presently encountered on the island (Engelskjøn 1986). One fruit of *Angelica* cf. *archangelica* is recorded in sample 30 of unit II (layer 11). Today this species has a more southern distribution with its northern limit in northernmost Norway. It grows on moist sandy or peaty soils, in willow shrubs, meadows and on river shores.

Three beetle species were identified among the insect remains (Table 6). The diving beetle *Agabus bipustulatus* is widespread in Europe. In arctic and alpine regions its main habitat is shallow lakes with stony or silty bottoms. The rove beetles *Olophrum boreale* and *Eucnecosum tenue* are distributed in northernmost Europe, where they are found in leaf litter of *Salix* and *Betula*. Caddis fly larvae (*Trichoptera*) of the family Limnephilidae occur in all sorts of habitats, ranging from fast-running streams to large lakes. Midge larvae (*Diptera*, Chironomidae) mainly live in the bottom sediments of lakes or ponds. The jaw of the notostracan crustacean *Lepidurus* (tadpole shrimp) found in unit II (layer 11, sample 31) could not be identified to species level. However, *Lepidurus articus* Pallas is a common species today north of the Arctic Circle, where it lives either in temporary pools or at the edges of lakes (Taylor & Coope 1985).

Chronostratigraphy

Serious problems concerned with the radiocarbon dating of arctic sediments have been reported in previous studies (e.g. Olsson 1986; Björck et al. 1994a, b; Abbott & Stafford 1995; Miller et al.

Table 6. Macroscopic remains of plants and animals from cores ST 2, 3A and 4. L = leaves, Bs = budscales, F = fruit, Ms = Meta/Mesosternum, LE = left elytron, RE = right elytron, Th = thorax, H = head, Mnd = jaw. Relative abundance of remains are indicated as + = 1–10, ++ = 11–100, +++ > 100. See Fig. 3 for the location of the samples.

TAXON	SAMPLES
SPERMATOPHYTA	
Salicaceae	
Salix reticulata L.	26, 29, 30, 32, 40 (L)
Salix herbacea L.	15, 34 (L)
Salix polaris Wahlenb.	10 (L)
Salix spp.	8–11 (Bs), 15 (Bs), 22, 23 (L), 26 (L), 27 (L, Bs), 30 (Bs), 38 (L)
Rosaceae	
Dryas sp.	11, 29 (L)
Apiaceae	
Angelica cf. *archangelica* L.	30 (F)
BRYOPHYTA indet.	6 (++), 8 (++), 9 (+), 10, 11 (++), 12, 14–16 (+), 18 (++), 19, 20 (+++), 21, 22 (++), 23–27 (+), 28 (++), 29–34 (+), 38–40 (+)
INSECTA	
Coleoptera	
Dytiscidae	
Agabus bipustulatus (L.)	11 (Ms)
Staphylinidae	
Olophrum boreale (Payk.)	8 (RE), 10, 13 (LE), 33 (Th)
Eucnecosum tenue (LeC.)	38 (RE)
Gen. indet.	30 (Ms)
Trichoptera	
Limnephilidae indet.	23, 27, 38 (Th)
Hymenoptera	
Fam. indet.	10, 31 (H)
Diptera	
Chironomidae indet.	4, 6, 8–13, 15–17 (+), 18–20 (++), 21 (+), 22–25 (++), 26, 27 (+), 28, 29 (++), 30 (+), 31 (++), 32–40 (+)
NOTOSTRACA	
Lepidurus sp.	31 (Mnd)

1995). The major problem in coal-bearing regions is that bulk sediment dates give erroneous ages due to "old carbon" derived from bedrock (Olsson 1968; Björck et al. 1994a). Another source of error may be ^{14}C-depleted organic carbon, which is stored in tundra environments and incorporated in the sediments at a later date (Abbot & Stafford 1995). To obtain correct radiocarbon dates, which exclude these sources of error, we only chose carefully selected macrofossils for dating. The selected samples contained >2 mg dried material. Two samples were composed of moss remains and two samples of leaves of *Salix* sp. (Table 7). The four AMS measurements obtained enable us to date the beginning of the organic production in the lake at the transition from unit I to unit II and the uppermost part of unit II (Fig. 3). To be able to compare our AMS dates to the bulk radiocarbon dates obtained earlier on Bjørnøya (Hyvärinen 1968, 1970; Olsson 1968), it was necessary to transform them into a bulk sediment age. If the organic carbon content and the age of the macrofossils in the sediment are known, as in this case (see Table 7 and Fig. 4), the influence of old bedrock carbon on bulk sediments can be calculated with the formula:

$$A_{org} = -8033 \ln \left[\frac{e^{\frac{-A_{bulk}}{8033}}}{x} \right]$$

where A_{org} = the macrofossil AMS ^{14}C measurement
A_{bulk} = the bulk ^{14}C age
x = the fraction C_{org} of C_{tot}

If this formula is applied to our dates (Table 7), the AMS ^{14}C ages of the samples would result in bulk ^{14}C ages of between 16,955 and 10,130 BP. In this example the contribution of 60–20% of "old carbon" causes age differences of between 7200 and 1800 radiocarbon years. The gradual decrease in the amount of minerogenic carbon in the younger sediments decreases the difference between the "true age" and the bulk age.

Three dates on sediment samples from Vestre Skinkevatnet (northern part of Bjørnøya), obtained on the humic fraction (extracted with 1% NaOH) were published by Hyvärinen (1968, 1970) and discussed by Olsson (1968). The lowermost date, Ua-2031 with an age of 11,200 ± 500 ^{14}C BP was obtained ca 10 cm below Hyvärinen's (1968) pollen zone transition I/II. Ua-2050 (in pollen zone IIb) gave an age of 4600 + 1200/−1000 ^{14}C BP. However, Ua-2049, ca 5 cm below the pollen zone transition II/III, gave an older age of 6000 + 3100/−2200 ^{14}C BP. In the case of sample Ua-2031 additional wet combustion with H_2O_2 and HNO_3 resulted in an age of 8300 + 1400/−1200 ^{14}C BP (Ua-2042). The non-dissolved remains were dated at 8900 + 1200/−1000 ^{14}C BP (Ua-2064) (Hyvärinen 1968; Olsson 1968). Olsson (1968) suggested that the discrepancies between the different fractions of the bulk sediment were caused by coal particles. The large errors and the age inversion of the two younger samples (Ua-2050, Ua-2049) indicate that too little humus could have been extracted for a measurement (Olsson 1968) which makes a comparison to our AMS dates impossible.

Based on the assumption that our local pollen zone SPZ 1 (5.62–5.52 m) in core ST 3A (Fig. 9) might be comparable to Hyvärinen's (1968) zone I, then our AMS ages of between ca 9800–9500 ^{14}C BP should correspond approximately to Hyvärinen's bulk age of 11,200 ± 500 ^{14}C BP (Ua-2031). If this correlation holds true, one might draw the conclusion that the amount of "old carbon" present in sample Ua-2031 is ca 15–20% which

Table 7 AMS ^{14}C measurements on plant macrofossils from cores ST 2 and ST 3A. The amount of bedrock carbon (C_{coal}) has been calculated from the carbon values of the corresponding layers. For the calculations of the bulk ^{14}C age BP, see formula in the text.

Lab. no. Ua-	Core layer no.	Depth (m)	Taxon	Sample weight before/after pre-treatment (mg)	AMS ^{14}C yrs BP	C_{coal} (%)	Bulk ^{14}C age BP
4800	ST 2/11	5.25–5.40	*Salix* (Leaves)	2.58/1.84	8340 ± 85	20	10,130
4799	ST 2/11	5.40–5.50	*Salix* (Leaves)	2.71/1.02	8340 ± 125	20	10,130
4131	ST 3A/9	5.50–5.58	*Bryophyta* indet.	–/24.27	9565 ± 95	30	12,430
4130	ST 3A/8	5.58–5.60	*Bryophyta* indet.	–/18.3	9795 ± 90	61	16,955

would result in a "true age" of ca 9650 ^{14}C BP. Such an age would then correspond to our age attribution for SPZ 1. However, this approach is highly hypothetical, because (1) the dates were performed on material from two different lakes and (2) we do not know the minerogenic carbon content of the old samples.

Palaeoenvironmental synthesis

Before 9800 ^{14}C BP

The highly minerogenic bottom layers (unit I) possess alternating coarse- and fine-grained sediments with a high concentration of redeposited coal particles. The lithology of these diamictons reflects the erosion of the surrounding bedrock. The compactness and the low water content, especially of the lower part of unit I (layers 1–4), implies over-consolidation. We suggest that these sediments were originally deposited as tills by a locally active glacier during the ice retreat (see also Salvigsen & Slettemark 1995), whereas the overlying sediments (layers 5–6) may originate from glaciofluvial/fluvial deposition.

As confirmed by the mineral magnetic analyses, the reddish-brown colour of the lowermost sediment is attributable to ferric oxides/oxyhydroxides, such as haematite and goethite, which are stable only in oxic environments (Berner 1971, 1981). The fact that this sediment was almost devoid of easily metabolised organic matter probably explains why it remained oxic after deposition, and why the ferric oxides survived. Few diatoms are found in this sediment which was probably deposited from a turbid water column, an inhospitable environment for living organisms. Oxic conditions after deposition may also have enhanced the corrosion and dissolution of the diatom valves.

The decreasing grain size, as well as the decrease in minerogenic carbon in the upper part of unit I, indicate that the erosion slowly ceased, possibly due to gradually more stable soils, which allowed deposition of a silty clay (Figs. 3 and 4). However, the transitions between the layers, and especially between layers 6 and 7, are sharp and may indicate active sediment resuspension and the formation of a subsequent hiatus. The pollen sample from layer 7 includes mainly long-transported pollen grains, but also suggests that *Salix* was growing in the surroundings. Algae of the type *Botryococcus*, mosses and midges found in the sediments indicate that the biological production in the lake had gradually started. Oxic conditions may also have prevailed during the deposition of the upper part of unit I, which is corroborated by the mineral magnetic analysis and explains why only so few (corroded) diatoms are present in the sediment.

9800–9500 ^{14}C BP

The transition from the minerogenic sediments in unit I to the organic sediments in unit II involves a drastic increase in the sulphur content and coincides with an abrupt change of the colour from reddish-grey to black (Figs. 3 and 4). The black sediment colour is derived from metastable sulphides of iron, in particular greigite (Fe_3S_4), the formation of which represents an arrested stage in pyrite diagenesis (Berner 1971, 1981). The microbial reduction of sulphate is a strictly anaerobic process, and the formation of greigite in sediments is intimately linked to the diagenetic processes associated with organic matter decomposition and the formation of H_2S. The bedrock of Bjørnøya and the Stevatnet catchment is rich in iron sulphides (e.g. pyrite) and iron oxides and is potentially a major source of both iron and sulphur. Another important source of sulphate must be sea spray, which is transported by winds over the island and deposited in the lakes. It seems therefore reasonable to assume that the availability of easily metabolised organic matter, rather than of sulphur or iron, was a limiting factor in the sulphide diagenesis. As a result, conditions which supported oxygen depletion and associated sulphide formation did not develop until reactive organic compounds were added to the sediment through the onset of biological production. This development coincides with an increase in the number of midges, moss remains and in *Pediastrum* in the sediment. Once the prerequisites were given, restricted exchange of oxygen due to long seasons of ice-cover may have further enhanced the oxygen depletion in the basin. Relatively harsh conditions and/or a high amount of clay in the water column may be the reason why diatoms are still rare in the sediments from this time period.

The pollen record is dominated by long-transported tree pollen. *Salix*, Ranunculaceae, Ericaceae and *Saxifraga* pollen may be regarded as local.

9500–8300 ^{14}C BP

The gradual increase in organic matter in the sediment during this period is probably due to a combination of enhanced production in the lake, development of pioneer plant communities and increased inwash of organic material from the surrounding catchment (see below).

Apart from midges, remains of *Coleoptera*, *Trichoptera* and *Hymenoptera* are found together with algae and mosses. The few diatoms present in the lower part of unit II indicate freshwater conditions and a slightly higher pH value than that which the top sample indicates. The low concentration of diatoms at 5.37 m could be related to a high clay content in the water column.

The pollen include long-distance transported tree and non-arboreal pollen. However, *Salix*, Rosaceae, Ericaceae, Ranunculaceae and *Saxifraga* may be regarded as local pollen producers. The vegetation in the close surroundings of the lake may have been composed of, among others, willow shrubs (*Salix reticulata*, *Salix polaris*) on well-drained grounds, of *Dryas* plants on calcareous soils and *Angelica* cf. *archangelica*, which grows on moist sandy or peaty soils or in willow scrub areas.

The climatic reconstruction using the MCR method is based on two beetle species, *Agabus bipustulatus* and *Olophrum boreale* recorded in samples 10 and 11 of unit II (Table 6). The results indicate a probable mean July temperature ($TMAX_{corr}$) of 9.3 ± 2°C and a mean January temperature ($TMIN_{corr}$) of −12.3 ± 5°C. A warmer climate during this time period than today is also suggested by the presence of the vascular plants *Dryas* sp. and *Angelica* cf. *archangelica*, which require higher summer temperatures than those prevailing on the island at present (Engelskjøn 1986). The MCR results from Stevatnet suggest thus 4–5°C higher mean July temperatures than present. The winters seem to have been slightly colder than present on Bjørnøya, with mean January temperatures 5–6°C lower than today.

A strong seasonality, which implies more continental conditions during this period, may explain some of the changes in the lake/catchment ecosystem that are recorded in the lake sediments. The formation of the distinctly sulphide laminated sediment in the upper part of unit II is connected to cyclic, possibly seasonal alterations of the redox conditions. The fact that the laminations are best preserved in core ST4, which was collected from the deepest part of the lake, implies that bottom anoxia developed during seasonal stratification of the lake or during periods of long ice cover. Furthermore, the preservation of these laminae suggests that bottom anoxia was severe enough to eliminate benthic animals, whose grazing and burrowing activities normally obliterate sediment structures. The increased summer temperatures must have enhanced thaw processes in the uppermost soil layers which explains the episodes of increased supply of allochthonous material, both minerogenic and organic.

8300 ^{14}C BP to present

There are no AMS ^{14}C dates available which would allow an age assignment for the silty gyttja clays in unit III. We can only assume that the sediments were deposited between 8300 ^{14}C BP and the present, which indicates that the sedimentation rate in general decreased considerably compared to the previous periods. During the deposition of the lower part of unit III rather calm conditions may have prevailed in the lake basin, followed by sporadic inwash of minerogenic material. In the upper part of unit III, a sudden drastic increase in grain size is accompanied by an increase in minerogenic and organic carbon and in the sulphur values. Increased in-wash of material from the surrounding slopes by soil processes/active weathering/freeze-thaw processes might be an explanation for this phenomenon.

Chironomidae and Limnephilidae are present among the limnic fauna, and shrubs of *Salix reticulata* and *Salix herbacea* grew in the lakes' surroundings. These plants are a preferred habitat for the two rove beetles *Olophrum boreale* and *Eucnecosum tenue*. Long-transported tree pollen increase gradually and non-arboreal pollen show a slight decrease. The benthic diatoms which are abundant in the top sample indicate that the lake has become slightly acid (possibly around pH 5–6).

Conclusions

The interpretation of our data set is based on lithology, grain size, mineral magnetic measurements, geochemistry, micro- and macrofossil analyses and AMS ^{14}C dates on plant macrofossils. This multi-disciplinary approach allows us

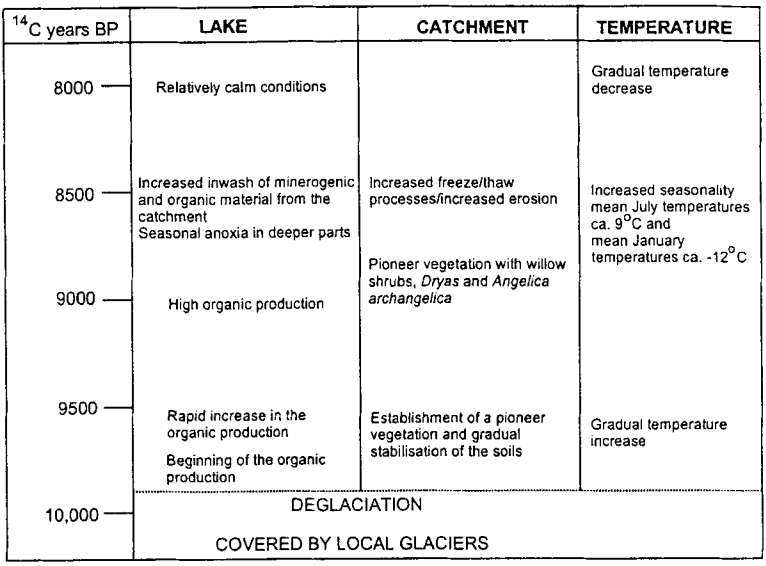

Fig. 10. A palaeo-environmental synthesis of the early Holocene palaeoenvironment on Bjørnøya based on the Stevatnet sequence.

to suggest a possible environmental scenario for the early Holocene on Bjørnøya, summarised in Fig. 10.

Immediately after large scale deglaciation and prior to ca 9800 ^{14}C BP, glacial sediments were deposited in the lake basin. The time period between 9800 and 9500 ^{14}C BP is characterised by gradually more stable soils, a very sudden increase in limnic production, although long seasons of snow and ice cover may have restricted an extensive development of the biological communities. The increase in limnic production coincides with the abrupt sea surface temperature rise of 2–3°C between ca 10,000 and 9500 ^{14}C BP (Hald & Dokken 1995) which was caused by the replacement of cold Arctic waters with warm Atlantic water in the western and southeastern Barents Sea (Hald & Vorren 1987; Vorren et al. 1988).

Between ca 9500 and 8300 ^{14}C BP a more continental climate, with strong seasonal contrasts prevailed on Bjørnøya. The marked temperature increase, with mean July temperatures around +9°C, is possibly as much as 4–5°C higher than present and the mean January temperatures around −12°C may have been 5–6°C lower than present. The plant communities on Svalbard show that high summer temperatures affect plant growth, mostly through the length of the snow-free growing season (Rønning 1969; Engelskjøn 1986; Skye 1989). High summer temperatures on Bjørnøya between 9500 and 8300 ^{14}C BP were responsible for the development of a pioneer community including *Dryas* and *Angelica archangelica*. As a consequence of the strong seasonality, freeze/thaw erosional processes in the surrounding soils must have been enhanced. This, in combination with the more extensive vegetation cover caused an increase in the deposition of allochthonous organic material in the lake. This increase, coupled with high autochthonous productivity in the lake during the summer months, may have caused oxygen deficiency, particularly severe during seasonal stratification and periods of ice cover. Rapid snow melt and an influx of a large quantity of water into the lake during the spring months would have caused temporary destratification and oxygenation of the sediments. This may explain why the lake experienced alternating oxic and anoxic conditions, indicated by the FeS laminated sediments and the precipitation of authigenic greigite (Hilton 1990).

Between 8300 ^{14}C BP and the present the sedimentation rate decreased considerably and apart from two periods which display an increased inwash of minerogenic and organic material, the lake basin experienced fairly calm sedimentation. Anoxic conditions coincided with the increase in total carbon content. The lack of ^{14}C dates makes it, however, impossible to discuss these phases in more detail. The diatoms in the top sediment indicate that the lake has become more acid.

Our temperature estimates for the time period

between 9500–8300 ^{14}C BP compare well with other studies from around the Kara, Laptev and East Siberian Seas, where a climatic optimum is described between 10,000–8500 ^{14}C BP (Verkulich et al. 1995) when arctic hunters seem to have migrated into these high altitudes (Pitulko & Makeyev 1991). Higher temperatures than present for the early Holocene are also recorded from several studies on Svalbard. Thermophilous marine molluscs flourished e.g. between ca 9500–4000 ^{14}C BP (Salvigsen et al. 1990, 1992) and the Linnébreen glacier melted completely during this period (Mangerud & Svendsen 1990). Temperature estimates based on plant macrofossil studies in west Spitsbergen indicate that between ca 8000 and 4000 ^{14}C BP the mean July temperature was ca 2°C higher than today (Birks 1991), which is slightly later than our "temperature optimum". Compared to our data this may suggest that temperature had already slightly decreased after 8000 ^{14}C BP, and that the warmest period during the early Holocene occurred around 9500 and 8300 ^{14}C BP, as recorded in the sediments recovered from Stevatnet. This coincides well with calculations of the solar radiation for the Northern Hemisphere which suggest that maximum Holocene seasonality was reached at around 9000 ^{14}C BP, with summer insolation higher and winter insolation lower than today (Kutzbach & Webb 1993). This pattern matches our environmental reconstruction convincingly well.

Acknowledgements. – Our thanks go to the Swedish Polar Secretariat and the Norwegian Polar Institute for logistic and economic support of the field work, to the Norwegian Coastal Guard, who arranged the transport to and from the island, to the staff at Radio Bjørnøya, whose great hospitality compensated for all the foggy and rainy days during the field work, to the helicopter crews of the Norwegian "Redningstjenesten" for their help with the transport of the fieldwork equipment and the spectacular flights over the island, to X. Bao (Lund) for the pollen preparations and the sulphur analyses on core ST 3B, to C. Peters (Edinburgh) for measuring the thermomagnetic properties, to M.-J. Gaillard (Lund) and H. Hyvärinen (Helsinki) for their help in interpreting the pollen diagram and to S. Björck (Copenhagen) and O. Bennike (Copenhagen) who critically read the manuscript and suggested many valuable improvements.

References

Abbott, M. B. & Stafford, T. W. 1995: Radiocarbon reservoir ages and carbon cycling in arctic and high-elevation lake systems. *Abstract, Second Annual PALE Research Meeting*, Eatonville, Washington, 4–6 February 1995.

Atkinson, T. C., Briffa, K. R., Coope, G. R., Joachim, J. M. & Perry, D. W. 1986: Climatic calibration of coleopteran data. Pp. 851–858 in Berglund, B. E. (ed.): *Handbook of Holocene Palaeoecology and Palaeohydrology*. Wiley, Chichester.

Atkinson, T. C., Briffa, K. R. & Coope, G. R. 1987: Seasonal temperatures in Britain during the past 22,000 years, reconstructed using beetle remains. *Nature 352*, 587–592.

Battarbee, R. W. (1986): Diatom analysis. Pp. 527–570 in Berglund, B. E. (ed.): *Handbook of Holocene Palaeoecology and Palaeohydrology*. Wiley, Chichester.

Berner, R. A. 1971: *Principles of chemical sedimentology*. McGraw-Hill Book Company. 240 pp.

Berner, R. A. 1981: A new chemical classification of sedimentary environments. *J. Sediment. Petrol. 51*, 359–365.

Birks, H. H. 1991: Holocene vegetational history and climatic change in west Spitsbergen-plant macrofossils from Skardtjørna, an Arctic lake. *The Holocene 1 (3)*, 209–218.

Björck, S., Bennike, O., Ingólfsson, I., Barnekow, L. & Penney, D. N. 1994a: Lake Boksehandsken's earliest postglacial sediments and their palaeoenvironmental implications, Jameson Land, East Greenland. *Boreas 23*, 459–472.

Björck, S., Wohlfarth, B., Bennike, O., Hjort, C. & Persson, T. 1994b: Revision of the early Holocene lake sediment based chronology and event stratigraphy on Hochstetter Forland, NE Greenland. *Boreas 23*, 513–523.

Bondevik, S., Mangerud, J., Ronnert, L. & Salvigsen, O. 1995: The postglacial sea-level history of Edgeøya and Barentsøya, eastern Svalbard. *Polar Res. 14(2)*, 153–180.

Elverhøi, A. & Solheim, A. 1983: The Barents Sea ice sheet – a sedimentological discussion. *Polar Res. 1 n. s.*, 23–42.

Elverhøi, A., Nyland-Berg, M., Russwurm, L. & Solheim, A. 1990: Late Weichselian ice recession in the central Barents Sea. Pp. 289–307 in Bleil, U. & Thiede, J. (eds): *Geological History of the Polar Oceans: Arctic Versus Antarctic*. Kluver Academic Publishers, Netherlands.

Elverhøi, A., Andersen, E., Dokken, T., Hebbeln, D., Spielhagen, R., Svendsen, J. I., Sørflaten, M., Rørnes, A., Hald, M. & Forsberg, C. F. 1995: The growth and decay of the Late Weichselian ice sheet in western Svalbard and adjacent areas based on provenance studies of the marine record. Abstract in Andrews, J. T., Austin, W. E. N. & Bergsten, H. E. (eds) *The Lateglacial Palaeoceanography of the North Atlantic Margins*. Edinburgh.

Engelskjøn, T. 1986: Eco-geographical relations of the Bjørnøya vascular flora, Svalbard. *Polar Res. 5*, 79–127.

Fitter, R. & Manuel, R. 1986: *Field Guide to the Freshwater Life of Britain and North-West Europe*. Collins, London, 382 pp.

Fleetwood, A., Pejler, B., Einsle, U. & Arnemo, R. 1974: Stratigraphical and biological investigations of some Bjørnøya lakes. *Norsk Polarinst. Årsbok 1972*, 63–71.

Hald, M. & Vorren, T. O. 1987: Stable isotope stratigraphy and palaeoceanography during the last deglaciation on the continental shelf off Troms, northern Norway. *Palaeoceanogr. 2(6)*, 583–599.

Hald, M. & Dokken, T. 1995: Palaeoceanography on the European Arctic margin during the last deglaciation. Abstract in Andrews, J. T., Austin, W. E. N. & Bergsten, H. E. (eds) *The Lateglacial Palaeoceanography of the North Atlantic Margins*. Edinburgh.

Hilton, J. 1990: Greigite and the magnetic properties of sediments. *Limnol. and Oceanogr., 35*, 509–520.

Hjelmroos, M. & Franzén, L. G. 1994: Implications of recent

long-distance pollen transport events for the interpretation of fossil pollen records in Fennoscandia. *Review of Palaeobot. Palynol. 82*, 175–189.

Hjort, C., Mangerud, J., Andrielsen, L., Bondevik, J. Y. & Salvigsen, O. 1995: Radiocarbon dated common mussels *Mytilus edulis* from eastern Svalbard and the Holocene climatic optimum. *Polar Res. 14(2)*, 239–243.

Horn, G. & Orvin, A. K. 1928: Geology of Bear Island. *Skr. Svalb. og ishav. 15*, 1–152, 9 pl., 1 geol map.

Hultén, E. & Fries, M. 1986: *Atlas of North European Vascular Plants*, Vol I–III. Koeltz Scientific Books, Königstein. 1172 pp.

Hyvärinen, H. 1968: Late-Quaternary sediment cores from lakes on Bjørnøya. *Geogr. Ann. 50A*, 235–245.

Hyvärinen, H. 1970: Flandrian pollen diagrams from Svalbard. *Geogr. Ann. 52A*, 213–222.

Kutzbach, J. E. & Webb III, T. 1993: Conceptual basis for understanding Late-Quaternary climates. Pp. 5–11 in Wright, H. E., Kutzbach, J. E., Webb III, T., Ruddiman, W. F., Street-Perrott, F. A. & Bartlein, P. J. (eds): *Global Climates since the Last Glacial Maximum*. University of Minnesota Press, Minneapolis.

Keilhau, B. M. 1831: *Reise i Øst- og Vest-Finmarken samt til Beeren-Eiland og Spitsbergen, i Aarene 1827 og 1828*. Christiania. 247 pp., 1 map, 3 pl. (Facsimile Børsums forlag, Oslo 1973).

Mangerud, J. & Svendsen, J. I. 1990: Deglaciation chronology inferred from marine sediments in a proglacial lake basin, western Spitsbergen, Svalbard. *Boreas 19*, 249–272.

McQuaker, N. R. & Fung, T. 1975: Determination of total sulfur and total phosphorous in soils using fusion with alkali metal nitrates. *Anal. Chem. 47*, 1462–1464.

Miller, G. H., Stafford, T. W. & Sauer, P. E. 1995: Radiocarbon dating arctic lake sediments. Abstract, *Second Annual PALE Research Meeting*, Eatonville, Washington, 4–6 February 1995.

Mossberg, B., Stenberg, L. & Ericsson, S. 1992: *Den nordiska floran*. Wahlström & Widstrand, Stockholm. 696 pp.

Nilsson, A. N. & Persson, S. 1989: The distribution of predaceous diving beetles (Coleoptera: Noteridae, Dytiscidae) in Sweden. *Entomol. Basiliensia 13*, 59–146.

Olsson, I. 1968: Radiocarbon analyses of lake sediment samples from Bjørnøya. *Geogr. Ann., 50A*, 246–247.

Olsson, I. 1986: Radiometric dating. Pp. 273–312, in Berglund, B. E. (ed.): *Handbook of Holocene Palaeoecology and Palaeohydrology*. Wiley, Chichester.

Palm, T. 1948: Skalbaggar. Coleoptera. Kortvingar, Fam. Staphylinidae – Underfam. Micropeplinae, Phloeocharinae, Olisthaerinae, Proteininae, Omaliinae. *Svensk Insektfauna 9*, 1–133.

Pitulko, V. V. & Makeyev, V. M. 1991: Ancient arctic hunters. *Nature 349*, 349.

Rønning, O. I. 1969: Features of the ecology of some arctic Svalbard (Spitsbergen) plant communities. *Arct. Alp. Res. 1*, 29–44.

Rønning, O. I. 1979: *Svalbards flora*. Polarhåndbok nr. 1. Norsk Polarinstitutt, Oslo. 128 pp.

Salvigsen, O. 1981: Radiocarbon dated raised beaches in Kong Karls Land, Svalbard, and their consequences for the glacial history of the Barents Sea Area. *Geogr. Ann. 63A*, 283–291.

Salvigsen, O. & Slettemark, Ø. 1995: Post glaciation and sea levels on Bjørnøya, Svalbard. *Polar Research 14(2)*, 245–251.

Salvigsen, O., Elgersma, A., Hjort, C., Lagerlund, E., Liestøl, O. & Svensson, N.-O. 1990: Glacial history and shoreline displacement of Erdmannflya and Bohemanflya, Spitsbergen, Svalbard. *Polar Res. 8*, 261–273.

Salvigsen, O., Forman, S. L. & Miller, G. H. 1992: Thermophilous molluscs on Svalbard during the Holocene and their paleoclimatic implications. *Polar Res. 11*(1), 1–10.

Skye, E. 1989: Changes to the climate and flora of Hopen Island during the last 110 years. *Arctic 42*, 323–332.

Steffensen, E. 1969: The climate and its recent variations at the Norwegian Arctic stations. *Meteorol. Ann 5(8)*. 347 pp.

Steffensen, E. 1982: The climate at Norwegian Arctic stations. Det Norske Meterologiske Institutt. *Klima 5*, 3–44.

Snowball, I. 1991: Magnetic hysteresis properties of greigite (Fe_3S_4) and a new occurrence in Holocene sediments from Swedish Lappland. *Phys. Earth Planet. Inter. 68*, 32–40.

Snowball, I. & Thompson, R. 1990: A stable chemical remanence in Holocene sediments. J. *Geophys. Res. 95*, 4471–4479.

Stein, R., Nam, S., Schubert, C., Vogt, C., Fütterer, D. & Heinemeier, J. 1994: The last deglaciation event in the eastern central Arctic Ocean. *Science 264*, 692–696.

Stober, J. C. & Thompson, R. 1979: Palaeomagnetic secular variation studies of Finnish lake sediments and the carriers of remanence. *Earth Planet. Sci. Lett. 37*, 139–149.

Taylor, B. J. & Coope, G. R. 1985: Arthropods in the Quaternary of East Anglia – Their role as indices of local palaeoenvironments and regional palaeoclimates. *Mod. Geol. 9*, 159–185.

Verkulich, S. R., Bol'shiyanov, D. Y., Makeyev, V. M. & Anisimov, M. A. 1995: Investigations of the lakes and estuaries of the Arctic in the framework of palaeogeographical studies of the AARI. *Abstract, Second Annual PALE Research Meeting*, Eatonville, Washington, 4–6 February 1995.

Vorren, T. O. 1992: Glaciations of the Barents Sea – an overview. *Sveriges Geol. Undersök. Ca 81*, 367–371.

Vorren, T. O., Hald, M. & Lebesbye, E. 1988: Late Cenozoic environments in the Barents Sea. *Palaeoceanogr. 3(5)*, 601–612.

Worsley, D. & Edwards, M. B. 1976: The upper Palaeozoic succession of Bjørnøya. *Norsk Polarinst. Årbok 1971*, 17–34.